Factors Controlling Chemistry of Magmatic Spinel: an Empirical Study of Associated Olivine, Cr-spinel and Melt Inclusions from Primitive Rocks

Article *in* Journal of Petrology · April 2001

DOI: 10.1093/petrology/42.4.655 · Source: OAI

CITATIONS
817

READS
1,085

3 authors, including:

Vadim S. Kamenetsky
University of Tasmania
421 PUBLICATIONS **13,857** CITATIONS

SEE PROFILE

Sebastien Meffre
University of Tasmania
305 PUBLICATIONS **8,515** CITATIONS

SEE PROFILE

JOURNAL OF PETROLOGY | VOLUME 42 | NUMBER 4 | PAGES 655–671 | 2001

Factors Controlling Chemistry of Magmatic Spinel: an Empirical Study of Associated Olivine, Cr-spinel and Melt Inclusions from Primitive Rocks

VADIM S. KAMENETSKY*, ANTHONY J. CRAWFORD AND SEBASTIEN MEFFRE

SCHOOL OF EARTH SCIENCES AND CENTRE FOR ORE DEPOSIT RESEARCH, UNIVERSITY OF TASMANIA, GPO BOX 252-79, HOBART, TAS. 7001, AUSTRALIA

RECEIVED NOVEMBER 5, 1999; REVISED TYPESCRIPT ACCEPTED JUNE 16, 2000

Compositions of ~2500 spinel–olivine pairs and 400 melt inclusion–spinel pairs have been analysed from 36 igneous suites from oceanic, arc and intraplate tectonic settings. Our data confirm that Cr-spinel mg*-number is largely controlled by melt composition, but also influenced by octahedral site substitutions, and rate of cooling. Lavas quenched in submarine environments tend to have higher* mg*-number at a given* cr*-number than slowly cooled subaerial lavas and peridotites. Unlike* mg*-number, Cr-spinel Al_2O_3 and TiO_2 contents show good correlations with melt composition, with only limited post-entrapment modifications. Our data suggest that increased activity of Al_2O_3 decreases the partitioning of TiO_2 into spinels. The Al_2O_3 content of Cr-spinel is a useful guide to the degree of partial melting of mantle peridotites; however, this same relationship is obscured in volcanic rocks. Al_2O_3 contents of volcanic Cr-spinels are mostly determined by melt composition rather than mantle source composition. The data also suggest that most spinels from residual mantle peridotites can be readily differentiated from those hosted in volcanic rocks. Mantle peridotite spinel tend to have lower TiO_2 and higher Fe^{2+}/Fe^{3+} ratios than spinel from volcanic rocks. The spinel compositions in our database can be subdivided on the basis of tectonic setting and mode of occurrence using an Al_2O_3 vs TiO_2 diagram. A total of seven fields can be distinguished with varying degrees of overlap. This diagram can then be used to determine the tectonic setting of spinel from altered mafic igneous rocks such as serpentinites or meta-basalts, or detrital spinel in sandstones.*

KEY WORDS: *mantle; melt inclusions; olivine; spinel; volcanic rocks*

INTRODUCTION

Roeder (1994) succinctly reviewed detailed studies over the last 20 years of Cr-spinel in mafic and ultramafic rocks. These studies have shown that spinel compositions are a complex function of magma (and source peridotite) composition (e.g. Irvine, 1965, 1967; Evans & Frost, 1975; Fisk & Bence, 1980; Maurel & Maurel, 1982*a*, 1982*b*; Sack, 1982; Dick & Bullen, 1984; Allan *et al.*, 1988; Allan, 1992, 1994; Arai, 1992, 1994*b*), fO_2 (e.g. Hill & Roeder, 1974; Murck & Campbell, 1986; Ballhaus *et al.*, 1991; Roeder & Reynolds, 1991), crystallization temperature and cooling rate (e.g. Fisk & Bence, 1980; Ozawa, 1984; Sack & Ghiorso, 1991; Scowen *et al.*, 1991), and perhaps pressure (e.g. Sigurdsson & Schilling, 1976; Jaques & Green, 1980; Ballhaus *et al.*, 1991; Roeder & Reynolds, 1991). Compared with usually co-liquidus olivine in primitive magmas, Cr-spinel compositions offer the potential to decipher important petrogenetic aspects of such magmas, including information on source peridotite 'fertility' (e.g. Dick & Bullen, 1984; Arai, 1987, 1994*a*; Clynne & Borg, 1997), early stage magma mingling, before or during aggregation of melt batches in subvolcanic magma chambers (e.g. Allan *et al.*, 1988; Allan, 1992; Danyushevsky *et al.*, 1995; Kamenetsky & Crawford, 1998; Kamenetsky *et al.*, 1998) and subsequent shallow-level magma mixing (e.g. Sigurdsson, 1977; Natland *et al.*, 1983; Thy, 1983).

*Corresponding author. Fax: 61-3-62232547.
E-mail: Dima.Kamenetsky@utas.edu.au

Many of the studies referred to above reported Cr-spinel data in isolation from host olivine compositions. In this study, we summarize a wealth of new compositional data for coexisting chromites and olivines from a diverse range of primitive lavas, including those from large igneous province (LIP) basalts (flood basalts), oceanic intraplate basalts, mid-ocean ridge basalts (MORB), back-arc basin basalts (BABB), intra-oceanic arc basalts (including those of tholeiitic, calc-alkaline and shoshonitic affinities), and several primitive boninite suites. For some suites, we also report analyses of melt inclusions in olivine and Cr-spinel hosts. Having analysed a statistically significant number (usually >50) of olivines from each lava, we are confident that we have identified the most high-Mg olivines crystallizing from each suite, so that the data presented are believed to be representative of the full crystallization range of Cr-spinel in these suites. To facilitate comparison and interpretation of the magmatic Cr-spinel data, we also present new data for several important ophiolitic peridotite suites, including those from the refractory harzburgitic New Caledonian ophiolite, and from *in situ* oceanic crust of Macquarie Island in the Southern Ocean.

These new data allow us to re-evaluate the spectrum of chromite compositions recorded from diverse tectonic settings, and to provide a more robust assessment of the significance of Cr-spinel composition variations than is often provided (usually based solely on Cr-spinel Cr/[Cr + Al] vs Fe^{2+}/[Mg + Fe^{2+}] values). Following the suggestion by Arai (1992), we apply the database and new compositional discriminant plots presented herein to interpret the origin and significance of spinels in sandstones and altered rocks from the Palaeozoic foldbelt in eastern Australia.

SAMPLE DESCRIPTION AND ANALYTICAL TECHNIQUES

Petrological criteria for choosing rock suites

Chromian spinel (hereafter 'spinel') is mainly present as inclusions in silicate minerals and less commonly it forms phenocrysts. For this study of spinel compositions we have chosen samples that satisfy the following requirements:

(1) all rock samples have volcanic origin, i.e. they are relatively rapidly quenched submarine or subaerial lava flows and tuffs or thin dykes with chilled margins. The rocks are fresh to moderately fresh. The choice of samples eliminates, as far as possible, the effects of post-entrapment modification of spinel compositions as a result of re-equilibration or alteration.

(2) The volcanics are representative of the different magma types occurring in well-constrained tectonic environments, namely, mid-ocean ridges (MORB), back-arc spreading centres (BABB), ocean islands (ocean-island basalt; OIB), continental rifts (LIP) and a variety of island-arc settings. Because of the large geochemical and petrological diversity of island-arc magmatism, different subtypes—boninitic, tholeiitic, calc-alkaline and high-K (shoshonitic) series—are considered separately.

(3) Within each magmatic series the most primitive compositions (the highest *mg*-number, i.e. Mg/[Mg + Fe^{2+}], and Cr and Ni contents) have been studied to ensure the presence of olivine phenocrysts hosting spinel inclusions. Although other phenocrysts may enclose spinel inclusions during cotectic crystallization (orthopyroxene, clinopyroxene and plagioclase), we favour the study of spinel trapped in olivine. The reasons are as follows: (a) olivine is the earliest phase to crystallize from virtually all mantle-derived melts; (b) olivine remains on the liquidus at least as long as spinel crystallizes; (c) olivine compositions (Fo, Ca, Ni) can be used as an indicator of the degree of magma fractionation; (d) the effects of olivine–spinel post-entrapment Mg–Fe^{2+} exchange can be evaluated; (e) olivine effectively armours enclosed spinel inclusions from other post-entrapment modifications (e.g. Scowen *et al.*, 1991).

(4) For each magmatic suite the compositional range of olivine was thoroughly studied to guarantee that the most primitive spinels, as well as spinel compositions along the liquid line of descent, are included in the database.

A complete set of rock samples used in this study is listed in Table 1 and their locations are shown in Fig. 1. The relevant petrological and geochemical information on the rock suites may be found in publications cited in Table 1. The abundance of olivine phenocrysts in these rocks is rather variable (from a few percent to 40–50 vol. %), and hence the rocks' MgO contents vary proportionally from ~6 to ~40 wt %. The range in the composition of olivine cores (Table 1), sometimes very large (10–15 mol % Fo) even within a single sample, suggests that none of the studied rocks represents a true melt composition. Therefore, we regard these porphyritic rocks as a mechanical mixture of olivine and other silicate phenocrysts when present (e.g. plagioclase and clinopyroxene in MORB, clinopyroxene in arc volcanics, and low-Ca pyroxene in boninites) and a residual melt (groundmass).The most Fe-rich olivines are usually in equilibrium with the groundmass composition, whereas more forsteritic olivines crystallized from more primitive melts at higher temperature, and were incorporated in the magma not long before the eruption. Olivine phenocrysts with their spinel and melt inclusions remain largely unequilibrated with the transporting melt, and thus offer snapshots of the preceding magmatic evolution.

Table 1: Geographic locations of studied samples and main compositional features of coexisting olivine and spinel

Suite no.	Locality	Reference†	Olivine, Fo	Spinel (compositional range)			
				mg-no.	*cr*-no.	TiO_2	Fe^{2+}/Fe^{3+}‡
Mid-ocean ridge basalts (MORB)							
1	15°20′N FZ, MAR	Dmitriev *et al.* (1991)	87·3–89·2	65–71	41–51	0·3–0·6	1·8–2·2
2	FAMOUS area, MAR	Langmuir *et al.* (1977); Kamenetsky (1996)	88·3–92·0	68–79	28–56	0·1–0·4	2·2–4·4
3	54°S, MAR	le Roex *et al.* (1987)	88·9–91·5	69–81	24–49	0·1–0·5	1·8–4·0
4	43°N, MAR	Shibata *et al.* (1979); Kamenetsky & Crawford (1998); Kamenetsky *et al.* (1998)	87·4–91·6	57–79	33–71	0·2–4·1	1·5–3·6
5*	Lamont seamounts, EPR	Allan *et al.* (1988)	88–91	66–84	20–54	0·2–0·9	1·2–1·9
6	Macquarie Island, SW Pacific	Kamenetsky *et al.* (2000)	84·2–90·4	55–77	26–59	0·3–1·5	1·4–3·1
Back-arc basins (BABB)							
7	North Fiji Basin	Sigurdsson *et al.* (1993)	88·2–90·0	72–78	23–37	0·3–0·5	2·0–2·6
8	Manus Basin	Dril *et al.* (1997)	83·2–91·4	45–77	25–84	0·1–0·9	0·7–2·4
9	Woodlark Basin	Dril *et al.* (1997)	88·3–90·0	62–78	25–62	0·3–0·8	1·3–2·0
10	Vanuatu back-arc troughs	Maillet *et al.* (1995)	76·2–91·4	25–77	17–84	0·1–3·2	0·7–3·0
11	Okinawa trough	Shinjo *et al.* (1999)	85·5–86·8	58–63	44–46	0·5–0·9	1·6–1·8
12	Lau Basin (Valu Fa Ridge)	Kamenetsky *et al.* (1997)	79·1–93·8	37–74	67–86	0·2–0·8	1·4–3·6
Island arc high-K and calc-alkaline series							
13	East Kamchatka (Valaginsky, Tumrok)	Kamenetsky *et al.* (1995*b*)	84·7–94·3	33–74	67–87	0·2–1·0	0·6–1·6
14	Roman Comagmatic Province (Montefiascone, Latium)	Kamenetsky *et al.* (1995*a*)	89·8–92·6	62–70	63–83	0·4–1·0	1·7–4·0
15	Aeolian arc (Vulcano, Lipari)	Kamenetsky & Clocchiatti (1996); Gioncada *et al.* (1998)	87·3–90·5	46–60	76–81	0·4–0·7	0·9–2·4
16	Vanuatu (Ambae)	Eggins (1993)	81·9–93·4	34–72	43–81	0·3–1·7	0·8–1·9
17	Vanuatu (Ambrym)	Picard *et al.* (1995)	85·1–93·8	34–71	83–91	0·2–0·5	1·4–3·7
Island-arc boninitic and tholeiitic series							
18	Howqua, Victoria (boninite)	Crawford (1980)	93·6–94·8	61–78	97–98	0–0·04	2·0–3·3
19	Cape Vogel, PNG (boninite)	Walker & Cameron (1983)	92·0–94·1	65–79	89–95	0–0·2	2·1–4·0
20	Hunter Ridge–Hunter FZ boninites	Sigurdsson *et al.* (1993)	85·2–92·2	47–69	72–90	0–0·4	1·3–4·1
21	Hunter Ridge–Hunter FZ tholeiites	Sigurdsson *et al.* (1993)	80·5–94·3	38–77	39–87	0·1–0·5	1·0–2·8
22	Troodos Upper Pillow Lavas (boninites)	Sobolev *et al.* (1993)	88·4–93·4	60–74	67–80	0·2–0·4	1·7–2·9
23	Vanuatu (Tanna) tholeiite	Monzier *et al.* (1997)	82·1–92·3	40–64	82–87	0·2–0·3	1·9–3·8
24	South Vanuatu seamounts high-Mg andesites	Monzier *et al.* (1993)	80·9–94·5	34–79	50–81	0·2–1·4	0·6–2·2
25	New Caledonia boninites	Cameron (1989)	88·5–93·6	56–75	83–87	0·1–0·3	2·2–3·4
Ocean-island basalts (OIB)							
26	Hawaii (Kilauea, Mauna Loa, Mauna Kea)	Sobolev & Nikogosian (1994)	76·9–90·1	36–68	49–73	1·1–3·3	1·2–2·7
27	Reunion	Sobolev & Nikogosian (1994)	79·8–88·9	40–62	57–65	1·5–7·5	1·6–2·9
28	French Polynesia (Tubuai, Mangaia)	Maury *et al.* (1994); Woodhead (1996)	77·9–86·6	24–56	42–66	1·5–15	0·9–2·2
Large Igneous Provinces (LIP)							
29	Karoo, South Africa	Bristow (1984)	85·4–88·3	40–54	72–84	3·2–4·4	2·5–3·6
30	Emeishan, SW China	Chung & Jahn (1995)	80·4–88·1	30–49	69–76	1·9–6·8	1·4–2·6
31	Central Siberian Plateau	Sobolev *et al.* (1992)	87·0–92·6	49–70	79–86	3·1–5·3	1·0–1·8
32	West Greenland, Disko Island	Holm *et al.* (1993); Lightfoot *et al.* (1997)	86·0–92·7	56–76	44–63	0·7–1·1	1·4–2·3
Mantle peridotites							
33	Macquarie Island, SW Pacific	Basylev & Kamenetsky (1998)	90·5–91·5	46–72	28–62	0–0·25	2·5–6·6
34*	Mid-ocean ridges	Dick (1989)	89·3–91·0	54–83	11–53	0–0·8	1·9–8·3
35*	Izu–Mariana forearc, Leg 125	Ishii *et al.* (1992)	90·5–94·0	27–68	31–87	0·06–0·25	>2·6
36	New Caledonia	Leblanc (1995)	88·4–92·6	38–72	31–74	0–0·3	2·6–9·7

*Suites for which we used published data on mineralogy.
†References contain general information on petrology, mineralogy and geochemistry of rocks.
‡Fe_2O_3 is calculated on the basis of spinel stoichiometry.

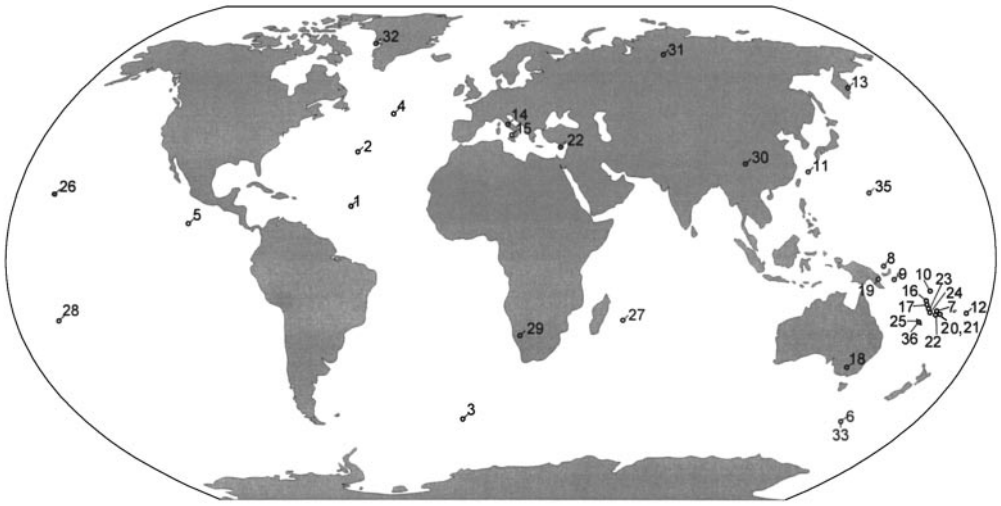

Fig. 1. Map showing the geographic position of studied suites. (For suite numbers see Table 1.)

The ranges in olivine Fo content in the studied rocks (Table 1) extend to the highest values recorded for a given type of magmatism. The presence in our collection of olivine Fo_{92} (mid-ocean ridges), Fo_{90} (ocean islands), Fo_{93} (continental rifts), $Fo_{94\cdot5}$ (island arcs), and $Fo_{93\cdot5}$ (back-arc basins) is good evidence for crystallization from high-temperature mantle-derived melts. It is worth noting that the composition of olivine (Fo) may be used as a measure of liquidus temperature and melt MgO only within a given magma series (e.g. MORB), whereas across the various magma series considered here, olivines of similar forsteritic content crystallize at very different temperatures (see Fo vs temperature plot in Sobolev & Nikogosian, 1994; Kamenetsky *et al.*, 1995*a*). For example, the liquidus temperature of Fo_{92} in MORB melt (FAMOUS area) is ~1300°C (Kamenetsky, 1996), whereas in the Siberian meimechite magma Fo_{92} crystallized at ~1560°C (Sobolev *et al.*, 1992). The MgO content of their parental melts is, therefore, also different (13·5 and 27 wt %, respectively), reflecting different melt Fe^{2+} contents.

To compare compositions of volcanic spinels with those from mantle peridotites we use published mineral analyses from oceanic peridotites worldwide (Dick, 1989), from the Izu–Mariana forearc, Leg 125 (Ishii *et al.*, 1992), and our data for Macquarie Island and New Caledonia peridotites. Information on the composition of melts parental to spinel in a number of samples was also obtained from the study of melt inclusions trapped in either spinel or olivine phenocrysts.

Spinel inclusions in olivine

Spinel inclusions are found in olivine phenocrysts from all magma types, but the abundance of spinel is highly variable. Some phenocrysts may contain numerous swarms of 5–6 to several tens of inclusions (typically in boninites), but more often they host either only occasional individual grains (e.g. North Fiji back-arc basalts), or the majority of olivines are devoid of any inclusions (e.g. Kamchatka high-K picrites).

Spinel inclusions are always octahedral, varying in size from several micrometres (in boninites and arc tholeiites) to 0·5 mm (in MORB and OIB). The colour of spinels in thin sections and brightness in reflected light depend on chemical composition, e.g. Fe–Ti-rich spinels are the brightest and almost opaque, Cr-rich spinels are translucent reddish brown to yellow–brown, and Al-rich spinels are the least reflective, greenish yellow to dull green in colour.

Melt inclusions in spinel and olivine

Melt inclusions, consisting of residual glass and daughter silicate crystals, are very common in spinel and olivine phenocrysts. Homogenization experiments with the melt inclusions were performed using a heating stage designed in the Vernadsky Institute of Geochemistry, Moscow (Sobolev *et al.*, 1980). The details of experimental procedure and compositions of individual inclusions and their host minerals from some suites that are discussed in this paper can be found in our (Zlobin *et al.*, 1991; Sobolev *et al.*, 1992, 1995; Kamenetsky *et al.*, 1993, 1995*a*, 1995*b*, 1997, 1998; Kamenetsky, 1996; Kamenetsky & Crawford, 1998) and other (Danyushevsky *et al.*, 1987; Gurenko *et al.*, 1992; Sobolev & Nikogosian, 1994; McNeill, 1997; Gioncada *et al.*, 1998) publications.

Sample preparation and analysis

The samples were crushed and sieved, and 50–200 olivine phenocrysts (0·3–1 mm) from each sample were hand picked, mounted in epoxy mounts, exposed and polished. Spinel inclusions in olivine grains in these mounts were marked for analysis. Similar mounts were prepared with spinel and olivine grains containing homogenized melt inclusions. Spinel and glass inclusions were analysed together with their host minerals by electron microprobe at the University of Tasmania and University of Paris VI (Cameca SX-50) and Vernadsky Institute of Geochemistry, Moscow (Camebax microbeam), using wavelength-dispersive spectrometry at 15 kV. Mineral (San Carlos olivine USNM 111312/444 and Cr-spinel UV-126) and glass (VG2—USNM 111249/52) secondary standards were analysed before and after each run, and 2–5 analytical points were used to calculate average composition. At least 25 grains of olivine and five spinels were studied in each sample. Host olivine was analysed not further than 20 μm from the spinel inclusions. The large number of analyses of individual olivine grains allowed determination of the entire range of olivine compositions, so that analyses of spinels were selectively performed on grains trapped in olivines over a wide range of Fo contents.

RESULTS AND DISCUSSION

The main compositional features of studied spinels (*mg*-number, *cr*-number = Cr/[Cr + Al], TiO_2, and Fe^{2+}/Fe^{3+}) are given in Table 1. The compositions of individual spinel inclusions trapped in the most primitive olivines are presented in Table 2. Below we discuss petrological aspects of the spinel compositional range in the lavas studied.

Olivine–spinel *mg*-number compositional relationships: the effects of crystallization and re-equilibration

The presence of spinel inclusions in olivine over a wide Fo range, including the most evolved olivines (e.g. $Fo_{75–80}$ in OIB) within a given sample or magma type, argues for continuous spinel crystallization together with the cotectic silicate phases other than olivine (pyroxenes and plagioclase) over a significant range of temperatures. In some cases (see Table 1 for the suites with the largest ranges of Fo) the crystallization temperature interval may exceed 200–250°C. Given the well-established early crystallization of pyroxenes in many island-arc (e.g. Barsdell, 1988; Eggins, 1993; Sobolev & Danyushevsky, 1994; Della-Pasqua *et al.*, 1995; Kamenetsky *et al.*, 1995*a*, 1995*b*, 1997; Della-Pasqua & Varne, 1997) and some MORB magmas (e.g. Kamenetsky *et al.*, 1998), and early crystallization of plagioclase in most MORB (e.g. Allan *et al.*, 1988; McNeill, 1997), as well as presence of spinel inclusions in pyroxene and plagioclase phenocrysts (this study), earlier claims that spinel crystallizes over a narrow temperature interval (Hill & Roeder, 1974; Fisk & Bence, 1980) and ceases to crystallize shortly after the appearance of clinopyroxene and plagioclase (Irvine, 1965, 1967; Dick & Bullen, 1984) seem to be unjustified.

Fractional crystallization (decreasing melt *mg*-number and temperature) should lead to related change in the *mg*-number of co-crystallizing olivine and spinel. For example, the observed positive correlation between olivine Fo and spinel *mg*-number in a given sample or suite (Fig. 2) reflects local equilibrium between these phases. The temperatures of olivine–spinel equilibria, calculated using the Ballhaus *et al.* (1991) model, are presented in the caption to Fig. 2. However, these temperatures ($T_{average}$ = 1067 ± 65°C for 650 olivine–spinel pairs shown in Fig. 2) correlate neither with Fo nor with real liquidus temperatures, and are in fact the closure temperatures for the Fe–Mg exchange between host olivines and spinel inclusions. The decrease in primary *mg*-number values of spinel inclusions in olivine as a result of re-equilibration at temperatures below liquidus (Irvine, 1967; Dick & Bullen, 1984; Ozawa, 1984; Ballhaus *et al.*, 1991; Scowen *et al.*, 1991) does not, however, obliterate correlations between *mg*-number and Fo in many volcanic suites (Fig. 2). On the other hand, the dispersion in spinel *mg*-number at a given Fo value, either within a given sample or suite or between suites, is controlled by some other factors. One is the dependence of the Mg and Fe^{2+} partitioning between olivine and spinel on the relative activities of Cr and Al in spinel (Dick & Bullen, 1984) or, in other words, the substitution of Fe^{2+} and Cr for Mg and Al (Allan *et al.*, 1988). For example, Fig. 2 shows that spinel coexisting with olivine becomes more Mg rich with decreasing *cr*-number. The distribution coefficient $K_d = (Mg/Fe)_{olivine}/(Mg/Fe^{2+})_{spinel}$ varies significantly from 2·5 (*cr*-number 20–30) to 10–12 (*cr*-number 80–90). At a given spinel *cr*-number, the distribution coefficient either remains constant (Fig. 2a) or varies within up to 30% of its value (Fig. 2c).

To further examine the possible effects of low temperature re-equilibration of spinel in terms of its *mg*-number we compared the compositions of spinel from quenched (underwater eruption, e.g. MORB, BABB and some arc tholeiites and boninites) and relatively slowly cooled (subaerial eruption, e.g. OIB and high-K arc series) rocks (Fig. 3a and b). The data (grouped according to host olivine Fo composition and plotted on the *mg*-number–*cr*-number diagram) demonstrate that at a given spinel *cr*-number and olivine Fo, spinel *mg*-number values from subaerial lavas are slightly lower (by up to 10 mol %).

Table 2: Representative compositions of spinel inclusions trapped in the most primitive olivines found in the studied samples (see Table 1)

Suite no.	TiO_2	Al_2O_3	Fe_2O_3	FeO	MnO	MgO	Cr_2O_3	Total	*mg*-no.	*cr*-no.	Fe^{2+}/Fe^{3+}	Host olivine, Fo
2	0·27	26·55	4·31	9·15	0·12	17·63	41·39	99·43	77·44	51·12	2·36	92·0
3	0·19	35·76	3·77	9·48	0·17	18·36	32·72	100·44	77·54	38·03	2·79	91·5
3	0·08	46·42	3·72	8·57	0·11	20·19	21·95	101·03	80·78	24·08	2·56	91·4
4	0·48	17·11	4·93	11·30	0·16	15·15	49·67	98·79	70·49	66·07	2·55	91·3
7	0·30	41·26	4·29	9·51	0·00	19·14	25·58	100·08	78·20	29·37	2·47	90·0
8	0·17	12·59	6·10	12·76	0·11	13·93	54·53	100·19	66·05	74·39	2·32	91·4
9	0·69	32·15	6·67	10·98	0·16	17·06	30·66	98·37	73·48	39·01	1·83	90·0
10	0·40	16·38	8·58	13·07	0·24	13·74	46·20	98·61	65·21	65·42	1·69	91·3
12	0·30	6·71	6·75	9·65	0·21	15·04	59·99	98·64	73·54	85·70	1·59	93·8
13	0·24	6·56	10·25	9·56	0·20	15·36	57·76	99·93	74·12	85·52	1·04	94·3
13	0·47	11·53	23·31	12·17	0·14	14·13	37·33	99·08	67·43	68·47	0·58	92·9
14	0·55	16·15	5·33	12·34	0·18	14·66	50·53	99·72	67·93	67·74	2·57	91·9
16	0·43	12·31	10·26	10·52	0·08	15·54	51·44	100·58	72·48	73·71	1·14	93·4
17	0·46	7·93	8·03	11·80	0·13	14·00	56·64	98·99	67·90	82·73	1·63	93·8
18	0·01	1·05	3·53	8·69	0·06	15·45	71·59	100·38	76·02	97·86	2·74	94·8
19	0·02	3·10	3·53	8·03	0·13	15·60	69·00	99·41	77·59	93·73	2·53	94·0
20	0·02	7·53	4·72	12·66	0·05	13·17	60·73	98·88	64·96	84·40	2·98	92·2
21	0·17	10·07	5·96	10·28	0·19	15·47	57·73	99·87	72·85	79·36	1·92	94·1
22	0·22	11·83	4·68	10·84	0·20	15·19	56·91	99·87	71·41	76·34	2·57	93·4
23	0·26	7·42	7·78	13·16	0·18	12·93	57·90	99·63	63·65	83·96	1·88	92·3
24	0·18	10·22	6·28	9·02	0·25	15·71	57·58	99·25	75·64	79·08	1·60	94·4
25	0·16	7·52	4·33	10·91	0·00	14·46	62·49	99·88	70·26	84·79	2·80	93·6
26	1·84	16·95	7·05	13·78	0·21	14·54	45·25	99·62	65·29	64·17	2·17	90·1
27	1·55	16·19	8·17	14·78	0·15	13·69	45·42	99·95	62·29	65·30	2·01	88·9
28	1·48	15·49	10·20	17·72	0·26	11·72	43·89	100·76	54·11	65·53	1·93	86·6
29	4·43	11·52	8·34	18·61	0·22	12·11	44·43	99·64	53·72	72·13	2·48	88·3
30	1·92	10·67	8·02	19·12	0·15	10·17	48·95	98·99	48·67	75·48	2·65	88·1
30	4·95	9·01	12·30	22·49	0·25	9·80	41·72	100·53	43·71	75·64	2·03	86·3
31	4·02	6·79	11·77	14·23	0·13	14·32	48·30	99·56	64·22	82·67	1·34	92·6
32	0·69	20·59	5·46	9·70	0·09	16·76	46·04	99·32	75·50	60·00	1·97	92·7

This is consistent with statistically lower blocking temperatures for olivine–spinel re-equilibration in subaerial lavas ($T_{average} = 1050 \pm 70$°C; $n = 600$) in comparison with quenched volcanics ($T_{average} = 1077 \pm 58$°C; $n = 871$). The effects of even slower cooling and lower closure temperature ($T_{average} = 681 \pm 44$°C; $n = 296$) are most pronounced in the *mg*-number of spinel from mantle (ophiolite or abyssal) peridotites. Compositions of spinels associated with olivine $Fo_{88·5–94}$ from a number of oceanic (arc- and rift-related) peridotites are significantly offset to lower *mg*-number (by up to 25–30 mol %) from the trends observed in pillow lavas (Fig. 3c). This shift increases significantly with increasing spinel *cr*-number.

Spinel *mg*-number should be interpreted with caution, as it is a complex function of a number of factors, the most important of which are (1) *mg*-number of the parental melt; (2) partitioning of Al and Cr in spinel, and hence Al_2O_3 in the melt (see below); (3) Fe^{2+}/Fe^{3+} in the melt, and hence fO_2; (4) post-entrapment re-equilibration with silicate minerals, and hence the cooling rate and spinel grain size. Consideration of the kinetics of olivine–spinel Mg–Fe^{2+} interdiffusion (Ozawa, 1984) precludes significant subsolidus re-equilibration for rapidly cooled, submarine volcanics, as their cooling rates of 100–100 000°C/h provide insufficient time for re-equilibration at near-magmatic temperatures. This contrasts

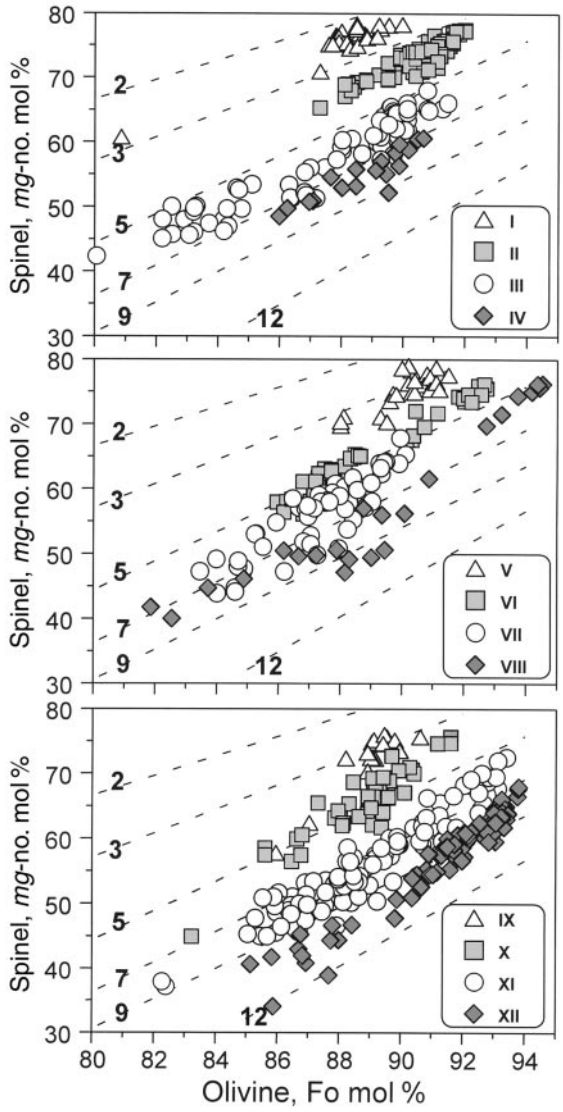

Fig. 2. Relationships between host olivine Fo and spinel inclusion *mg*-number. The compositional trends are presented for 12 populations (I–XII) of spinel compositions. Each population has a limited range in measured *cr*-number and olivine–spinel blocking temperature, calculated using the Ballhaus *et al.* (1991) geothermometer. (For suite numbers see Table 1.)

	I	II	III	IV	V	VI
Spinel *cr*-number	16–30	50–56	65–75	83–90	30–45	55–63
$T_{ol\text{–}sp} \pm \delta$ (°C)	1122 ± 50	1114 ± 38	1061 ± 28	1066 ± 27	1108 ± 67	1094 ± 32
Suite number	7–10	1, 2, 4	8, 10, 12	20	1–4	32
	VII	VIII	IX	X	XI	XII
Spinel *cr*-number	64–74	75–81	35–45	50–60	70–80	83–90
$T_{ol\text{–}sp} \pm \delta$ (°C)	1099 ± 68	1048 ± 71	1096 ± 57	1077 ± 54	1056 ± 49	963 ± 37
Suite number	26	24	7–10	8–10	16	17

Distribution coefficient $K_d = (Mg/Fe)_{olivine}/(Mg/Fe^{2+})_{spinel}$ values and isopleths of K_d (dashed lines) are shown.

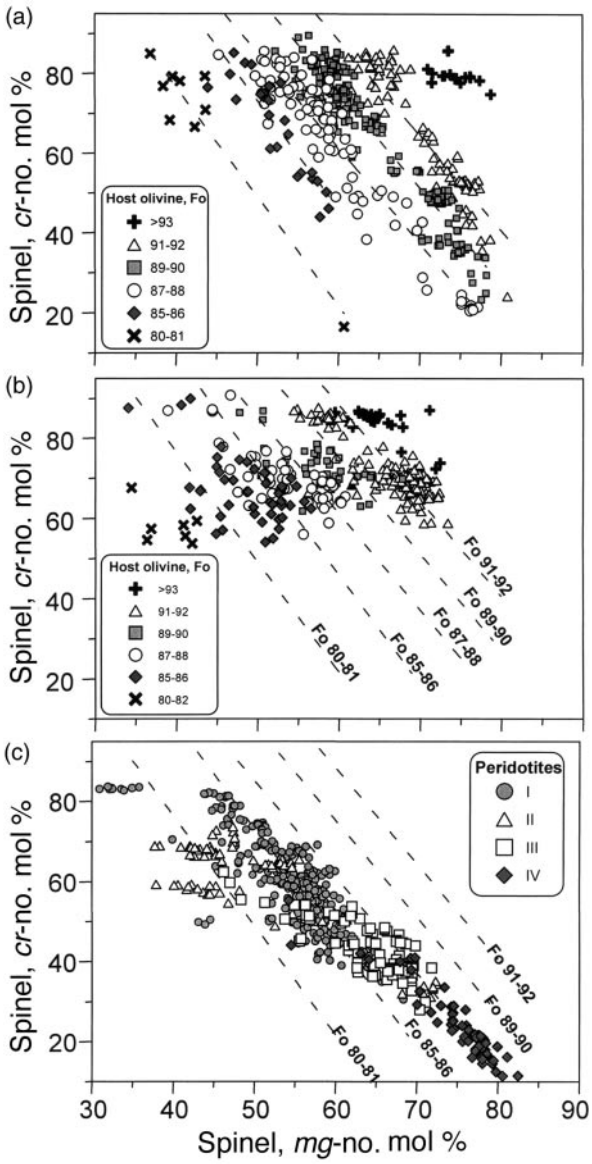

Fig. 3. Relationships between *mg*-number and *cr*-number in spinels from recent and modern submarine (a) and subaerial (b) rocks, and mantle peridotites (c). Peridotitic samples: I, Izu–Mariana forearc, Leg 125 (Ishii *et al.* (1992); II, New Caledonia; III, Macquarie Island; IV, variety of abyssal peridotites (Dick, 1989). Isopleths of olivine Fo (dashed lines) are calculated as a linear regression for olivine–spinel data from recent and modern submarine volcanics shown in (a).

with the rates of 0·1–0·001°C/h for slowly cooled subaerial thick lava flows, lava lakes, dykes and intrusive rocks, and thus the variable and extensive re-equilibration observed (Fig. 3b and c; Scowen *et al.*, 1991; Barnes, 1998). With respect to re-equilibration, Fo–*mg*-number or *mg*-number–*cr*-number correlations, even in submarine volcanics (Figs 2 and 3a), are not true liquidus relationships, as spinels trapped in more evolved olivine are likely to be re-equilibrated to a lesser extent than spinels hosted by more primitive, higher-temperature olivine. However, in this case Mg and Fe^{2+} exchange is considered to be minimal <5 mol % *mg*-number (Dick & Bullen, 1984; Allan *et al.*, 1988; Allan, 1994; Clynne & Borg, 1997), and the decrease in spinel *mg*-number, along with olivine Fo, is still a reflection of fractional crystallization. Figure 3a shows the isopleths of minimal Fo values of olivines hosting spinel of any *cr*-number value. This provides a useful estimate of olivine compositions in rocks where olivine is pervasively altered.

Spinel Al_2O_3 vs TiO_2: a guide to magma chemistry and tectonic provenance

Unlike Mg and Fe^{2+} in spinel trapped in olivine, magmatic abundances of trivalent (Al, Cr) and tetravalent (Ti) cations experience very little, if any, change during post-entrapment re-equilibration because of their low diffusivity in olivine (Roeder & Campbell, 1985; Scowen *et al.*, 1991; Barnes, 1998). To examine the effects of melt composition on the abundances of Al_2O_3 and TiO_2 in spinel, we use compositional pairs of spinel and glass coexisting as: (1) melt inclusions in spinels; (2) melt and spinel inclusions in the same olivine or olivines with similar Fo content; (3) spinel microphenocrysts in natural glass (Table 3).

A positive correlation between Al_2O_3 and TiO_2 contents in spinel and coexisting melt is demonstrated over significant intervals of averaged spinel and melt compositions (e.g. 3–39 and 4·6–18 wt % Al_2O_3, and 0·04–3·9 and 0·07–3·9 wt % TiO_2, respectively, see Fig. 4a and b and Table 3) sampled from a variety of magmatic types and tectonic environments. Similar covariations also exist even if more restricted compositional intervals represented by the individual samples or suites are considered (Fig. 4c and d). Our interpretation, concurring with other studies of natural rocks (e.g. Crawford, 1980; Dick & Bullen, 1984; Allan *et al.*, 1988; Arai, 1992; Della-Pasqua *et al.*, 1995; Kamenetsky, 1996) and compilation of experimental data (Danyushevsky, 1995), is that these relationships are primarily controlled by magmatic Al_2O_3 and TiO_2 abundances. The correlation of spinel and basaltic melt Al_2O_3 abundances, similar to that in Fig. 4a, has also been shown by experimental studies (Maurel & Maurel, 1982*a*; Roeder & Reynolds, 1991). The magma compositional control on spinel Al_2O_3, and the presence of Al-rich rims around Cr-rich cores in some spinel phenocrysts and inclusions in olivine (this study and Allan *et al.*, 1988; Allan, 1992; Della-Pasqua *et al.*, 1995) argue against the relatively high pressure of crystallization, which has been suggested to explain the rather aluminous (Al_2O_3 >40 wt %) composition of some spinels in MORB (e.g. Irvine, 1967; Sigurdsson & Schilling, 1976; Sigurdsson, 1977; Fisk & Bence, 1980). We also note that

Table 3: Average spinel and coexisting melt inclusion–glass compositions

Location (sample)/suite no.	Host	Reference	Spinel										
			TiO_2	Al_2O_3	Fe_2O_3	FeO	MnO	MgO	Cr_2O_3	Total	*mg*-no.	*cr*-no.	Fe^{2+}/Fe^{3+}
FAMOUS, MAR/2	spinel	this work; Kamenetsky (1996)	0·28	27·47	4·33	10·60	0·15	16·88	40·29	100·00	73·95	49·60	2·74
54°S, MAR/3	spinel	this work	0·23	31·07	4·31	10·58	0·08	17·06	35·59	98·92	74·17	43·49	2·75
54°S, MAR/3	olivine ($Fo_{89–91}$)	this work	0·20	34·85	4·29	9·94	0·11	17·96	32·83	100·19	76·27	38·88	2·62
43°N MAR (All 32 12-2)/4	spinel	this work; Kamenetsky & Crawford (1998)	0·39	20·84	4·36	11·17	0·11	15·75	47·04	99·66	71·54	60·26	2·92
43°N MAR (All 32 11-92)/4	spinel	this work; Kamenetsky & Crawford (1998)	0·51	19·41	4·99	11·15	0·13	15·65	47·70	99·53	71·44	62·25	2·49
Macquarie Island/6	spinel	this work	0·38	28·51	5·11	11·10	0·14	16·63	38·21	100·08	72·70	47·47	2·42
Macquarie Island (40428)/6	glass	this work; Kamenetsky *et al.* (2000)	1·47	20·91	9·23	16·49	0·18	12·48	36·99	97·75	57·43	54·27	1·98
Macquarie Island (60596)/6	glass	this work; Kamenetsky *et al.* (2000)	0·70	25·20	6·74	13·87	0·12	14·34	37·74	98·73	64·83	50·12	2·29
Macquarie Island (38324)/6	glass	this work; Kamenetsky *et al.* (2000)	1·26	25·21	9·34	14·51	0·09	14·15	33·69	98·25	63·48	47·27	1·73
Macquarie Island (38159)/6	glass	this work; Kamenetsky *et al.* (2000)	0·65	30·48	6·35	11·77	0·20	16·34	33·61	99·40	71·22	42·52	2·06
Macquarie Island (60701)/6	glass	this work; Kamenetsky *et al.* (2000)	0·56	33·58	5·89	11·45	0·12	16·86	30·84	99·30	72·41	38·13	2·17
Southern North Fiji Basin/7	olivine ($Fo_{89–90}$)	this work	0·41	35·96	5·16	10·69	0·14	17·81	29·87	100·04	74·82	35·79	2·31
E. Valu Fa Ridge, Lau Basin/12	olivine ($Fo_{>91}$)	Kamenetsky *et al.* (1997)	0·28	7·70	7·58	11·04	0·16	14·32	58·18	99·25	69·78	83·55	1·62
Tumrok, E. Kamchatka/13	spinel	Kamenetsky *et al.* (1993, 1995*b*)	0·28	10·93	10·51	12·03	0·18	13·71	50·86	98·49	66·96	75·78	1·27
Tumrok, E. Kamchatka/13	olivine ($Fo_{>91}$)	Kamenetsky *et al.* (1993, 1995*b*)	0·29	8·72	11·82	12·51	0·23	13·54	51·90	99·01	65·83	79·96	1·21
Valaginsky, E. Kamchatka/13	olivine ($Fo_{>91}$)	Kamenetsky *et al.* (1995*b*)	0·44	7·70	18·32	13·04	0·22	13·19	46·54	99·44	64·29	80·01	0·85
Vulsini, Roman Province/14	olivine ($Fo_{91–92}$)	Kamenetsky *et al.* (1995*a*)	0·49	15·34	6·08	12·29	0·22	14·59	50·96	99·98	67·90	69·04	2·29
Vulcano, Aeolian arc/15	olivine ($Fo_{89·5–90·5}$)	this work; Gioncada *et al.* (1998)	0·55	8·68	16·23	15·33	0·29	12·02	47·92	101·03	58·30	78·70	1·06
Cape Vogel, Papua New Guinea/19	spinel	this work	0·04	2·92	3·82	8·75	0·13	15·29	68·64	99·58	75·71	94·03	2·56
Hunter Ridge–Hunter FZ/20	spinel	this work	0·19	5·22	7·98	14·73	0·24	11·80	59·96	100·12	58·83	88·51	2·05
Karoo, South Africa/29	olivine ($Fo_{86–87}$)	this work	3·68	8·33	7·29	20·94	0·23	9·86	49·36	99·68	45·59	79·93	3·21
Emeishan, SW China/30	olivine ($Fo_{82–84}$)	this work	3·57	9·72	16·17	24·58	0·28	7·52	38·42	100·26	35·29	72·58	1·70
Central Siberia/31	olivine ($Fo_{90–92}$)	this work; Sobolev *et al.* (1992)	3·85	6·25	12·09	15·16	0·15	13·53	48·62	99·65	61·36	83·89	1·41
Nuussuaq, W. Greenland/32	glass	this work	0·97	18·57	9·55	16·22	0·28	12·27	40·91	98·78	57·43	59·64	1·89
Koryak highland, E. Russia	spinel	Zlobin *et al.* (1991)	0·08	10·37	5·00	13·16	0·21	13·40	57·79	100·02	64·49	78·89	2·95
Hunter Ridge–Hunter FZ	spinel	this work	1·00	24·92	7·86	15·36	0·25	13·88	36·90	100·17	61·69	49·83	2·17
Gorda Ridge, E. Pacific	spinel	McNeill (1997)	0·43	28·97	5·66	12·35	0·17	15·93	36·12	99·62	69·56	45·78	2·45
Hole 896A, E. Pacific	spinel	McNeill (1997)	0·36	29·10	6·33	11·65	0·16	16·40	36·01	100·00	71·48	45·44	2·05
Vema FZ, MAR	olivine (Fo_{90})	Danyushevsky *et al.* (1987)	0·16	38·96	5·64	8·72	0·13	19·12	26·79	99·52	79·62	31·57	1·72
Galapagos *Alvin* 1549-5	glass	this work	0·39	27·15	6·67	13·52	0·10	14·94	37·24	100·00	66·33	47·92	2·25
Galapagos All 60 9/20	glass	this work	0·33	36·71	4·82	10·06	0·13	18·29	30·49	100·82	76·42	35·79	2·32
Mauna Loa, Hawaii	spinel	Sobolev & Nikogosian (1994)	1·39	14·14	9·07	16·40	n.d.	12·24	45·85	99·09	57·06	68·47	2·03
Snæfellsnes, Iceland	olivine ($Fo_{88–89}$)	Gurenko *et al.* (1992)	0·91	23·67	7·74	13·94	0·19	14·60	38·40	99·44	65·13	52·10	2·01

Table 3: continued

	Melt											
	SiO_2	TiO_2	Al_2O_3	FeO	MnO	MgO	CaO	Na_2O	K_2O	P_2O_5	Cr_2O_3	Total
FAMOUS, MAR/2	49·32	0·61	15·41	7·81	0·14	10·72	13·08	1·55	0·08	0·07	1·16	99·95
54°S, MAR/3	50·92	0·61	15·17	4·85	0·11	10·91	13·66	1·57	0·06	0·05	0·71	98·60
54°S, MAR/3	50·25	0·61	16·60	5·79	0·09	11·11	13·08	1·48	0·04	0·08	0·07	99·19
43°N MAR (All 32 12-2)/4	50·47	0·77	14·48	6·81	0·13	10·68	13·08	1·67	0·34	0·11	0·91	99·46
43°N MAR (All 32 11-92)/4	51·39	0·99	14·41	6·92	n.d.	10·48	12·60	2·02	0·58	0·16	n.d.	99·56
Macquarie Island/6	50·71	0·85	16·58	6·42	n.d.	9·28	12·98	2·14	0·18	0·09	n.d.	99·24
Macquarie Island (40428)/6	50·40	1·68	15·89	9·10	0·16	6·84	10·84	3·10	0·58	0·29	0·08	98·95
Macquarie Island (60596)/6	50·56	1·52	15·91	8·35	0·14	7·12	12·13	2·76	0·58	0·28	0·05	99·40
Macquarie Island (38324)/6	49·39	1·75	15·88	8·54	0·13	6·75	10·92	1·88	0·79	0·32	0·08	96·42
Macquarie Island (38159)/6	48·77	1·48	17·22	8·32	0·13	8·15	11·94	2·91	0·49	0·22	0·02	99·66
Macquarie Island (60701)/6	49·09	1·37	16·99	7·68	0·12	8·02	12·63	2·72	0·59	0·23	0·05	99·50
Southern North Fiji Basin/7	49·49	1·29	17·72	7·17	n.d.	9·00	11·49	2·94	0·13	0·14	n.d.	99·36
E. Valu Fa Ridge, Lau Basin/12	50·23	0·44	9·08	7·83	n.d.	12·27	14·14	1·03	0·32	0·07	n.d.	95·42
Tumrok, E. Kamchatka/13	48·77	0·45	11·95	9·65	0·16	11·94	12·37	1·47	1·25	0·19	n.d.	98·20
Tumrok, E. Kamchatka/13	48·02	0·34	9·67	9·52	0·14	18·94	10·27	1·35	1·25	0·24	n.d.	99·74
Valaginsky, E. Kamchatka/13	48·95	0·54	9·00	9·98	0·09	16·58	9·7	1·86	2·54	0·47	n.d.	99·71
Vulsini, Roman Province/14	48·39	0·71	13·29	6·55	n.d.	9·22	13·44	1·30	3·99	0·31	n.d.	97·21
Vulcano, Aeolian arc/15	45·31	0·61	10·42	9·01	0·17	10·90	13·60	1·81	1·85	0·28	n.d.	93·96
Cape Vogel, Papua New Guinea/19	56·66	0·07	4·58	5·58	n.d.	27·39	2·55	0·29	0·08	0·02	n.d.	97·23
Hunter Ridge–Hunter FZ/20	51·36	0·32	7·95	10·23	0·29	12·87	10·44	0·43	0·26	0·05	1·74	95·94
Karoo, South Africa/29	52·01	3·25	9·08	9·75	0·07	13·37	6·35	1·63	2·89	0·56	0·16	99·11
Emeishan, SW China/30	47·45	3·04	9·61	13·76	0·15	12·09	10·03	2·16	0·82	0·22	0·13	99·46
Central Siberia/31	41·28	3·89	5·25	12·99	n.d.	23·20	9·20	1·69	1·36	0·58	n.d.	99·44
Nuussuaq, W. Greenland/32	48·56	1·84	14·69	10·87	0·15	7·99	13·09	2·13	0·24	0·19	0·01	99·76
Koryak highland, E. Russia	53·63	0·20	11·11	7·13	0·12	11·12	12·17	1·29	0·24	0·03	n.d.	97·04
Hunter Ridge–Hunter FZ	46·51	1·51	15·09	9·63	0·15	8·03	13·54	2·31	0·59	0·32	0·89	98·57
Gorda Ridge, E. Pacific	49·10	0·93	16·16	8·29	0·13	8·91	12·79	1·88	0·03	0·05	1·06	99·33
Hole 896A, E. Pacific	49·42	0·72	16·16	8·48	0·12	9·54	13·22	1·65	0·01	0·03	0·96	100·29
Vema FZ, MAR	53·70	0·34	17·04	6·65	0·15	6·69	13·96	1·44	0·03	n.d.	n.d.	100·00
Galapagos *Alvin* 1549-5	50·24	0·96	15·38	9·50	0·16	8·51	12·37	1·79	0·04	0·03	0·17	99·16
Galapagos All 60 9/20	51·24	1·00	17·99	7·15	0·11	7·05	13·26	2·21	0·06	0·07	0·03	100·16
Mauna Loa, Hawaii	49·16	2·19	11·93	11·55	0·21	13·55	9·15	1·75	0·32	0·19	n.d.	100·00
Snæfellsnes, Iceland	47·26	2·03	15·45	8·24	0·13	9·64	13·65	2·42	0·69	0·38	n.d.	99·87

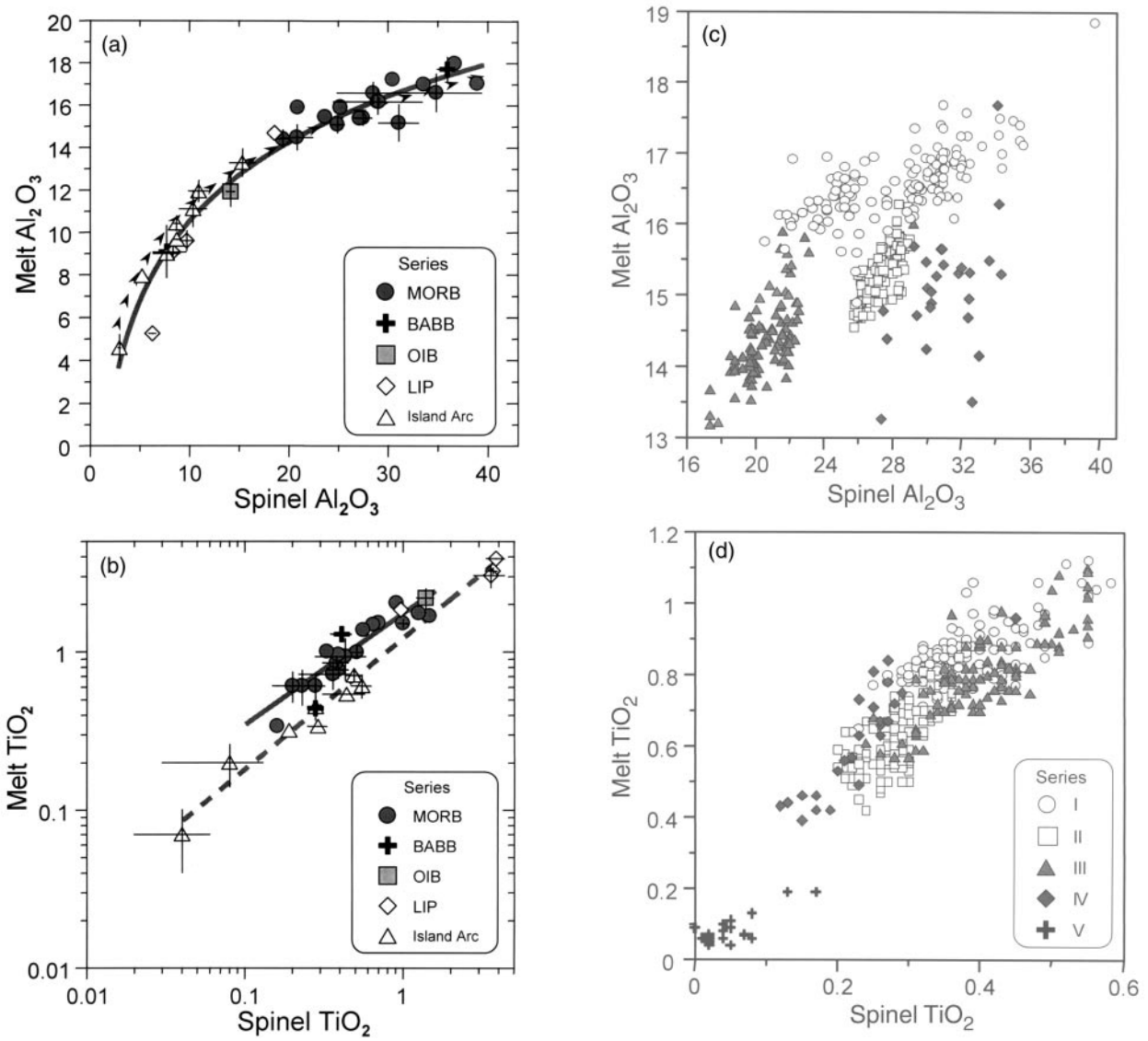

Fig. 4. Spinel–melt compositional relationships expressed in terms of Al_2O_3 and TiO_2 abundances (in wt %). (a, b) average compositions from Table 3. The error bar is equal to 1σ. Continuous line in (a) is a power best fit through all data; dashed arrowed line shows the correlation from the experimental study by Maurel & Maurel (1982*a*). Continuous and dashed lines in (b) are power best fits through the high-Al (Al_2O_3 in melt >14 wt % and in spinel >19 wt %) and low-Al (Al_2O_3 in melt <14 wt % and in spinel <15 wt %) compositions, respectively. (c, d) Melt inclusions and host spinel from individual suites: I, Macquarie Island; II, FAMOUS area, MAR; III, 43°N, MAR; IV, 54°S, MAR; V, Cape Vogel, Papua New Guinea.

despite a good correlation between TiO_2 in coexisting melt and spinel, low-Al spinel from the island-arc series and LIP are systematically more Ti rich at a given melt TiO_2. This implies that increasing Al activity in the system melt–spinel reduces the partitioning of Ti into spinel.

The dependence of spinel Al_2O_3 and TiO_2 concentrations on the parental melt composition (Fig. 4) suggests the use of an Al_2O_3 vs TiO_2 diagram to discriminate between spinels that crystallized from different magmas in different geodynamic settings (Fig. 5). Compositions of spinel coexisting with primitive olivine (Fo >84 mol %) from LIP, OIB, MORB [excluding uncommon for MORB high-Ti spinel from 43°N, Mid-Atlantic Ridge (Kamenetsky & Crawford, 1998)] and island-arc magmas form distinct fields with little overlap (Fig. 5a). The exception is spinel from modern back-arc environments, such as Valu Fa Ridge (Lau Basin), Vanuatu and Okinawa troughs, North Fiji, Manus and Woodlark basins. As expected by their transitional and

transient setting, back-arc spinel compositions spread across island-arc and MORB fields (Fig. 5b), reflecting the presence of subduction-related and MORB mantle and magma components and diverse melting conditions in this complex setting.

Island-arc spinels show far more significant overall and intra-sample variations in TiO_2 content than spinels in other magmas (Fig. 5c). These variations probably reflect the fact that parental magmas are also variable in TiO_2 as a result of mixing [e.g. with high-Ti OIB melts (Danyushevsky *et al.*, 1995)]. In general, arc spinel TiO_2 systematics is consistent with whole-rock chemistry and helps to distinguish between boninites–arc tholeiites, and calc-alkaline–high-K series, using a boundary at ~0·3–0·4 wt % TiO_2 (Fig. 5c).

Spinel Al_2O_3 (*cr*-number): inferences for mantle source and melting

Spinel *cr*-number (or Al_2O_3) values are commonly used to constrain the nature of the mantle peridotite source and the degree of partial melting (e.g. Jaques & Green, 1980; Duncan & Green, 1987; Bonatti & Michael, 1989). Although this is largely correct for mantle peridotites, as the compositional features of other minerals (e.g. olivine Fo, Al_2O_3 in pyroxenes) support trends in the spinel *cr*-number, the inferences for the parental mantle based on the *cr*-number of liquidus spinel could be misleading. The projection of *cr*-number in volcanic spinels onto the so-called Olivine–Spinel Mantle Array (Fo vs *cr*-number diagram; see Arai, 1987, 1994*a*) has been used in a number of petrological studies (e.g. Sigurdsson *et al.*, 1993; Arai, 1994*b*; Sobolev & Danyushevsky, 1994; Sobolev & Nikogosian, 1994; Kamenetsky & Clocchiatti, 1996). However, if this method is applied to compare mantle sources of magmas from flood basalt provinces with boninites or intraplate ocean-island magmas with island-arc tholeiites that all crystallized spinel with similar low Al_2O_3 (high *cr*-number), the conclusion should be that they have similar refractory, harzburgitic sources. On the other hand, mid-ocean ridge magmas that crystallize high-Al spinel, and are interpreted as products of multi-stage high-degree partial melting (Danyushevsky *et al.*, 1987; Sobolev & Shimizu, 1993), should, according to Arai's method, be derived from an undepleted lherzolitic mantle source. This is clearly in conflict with other

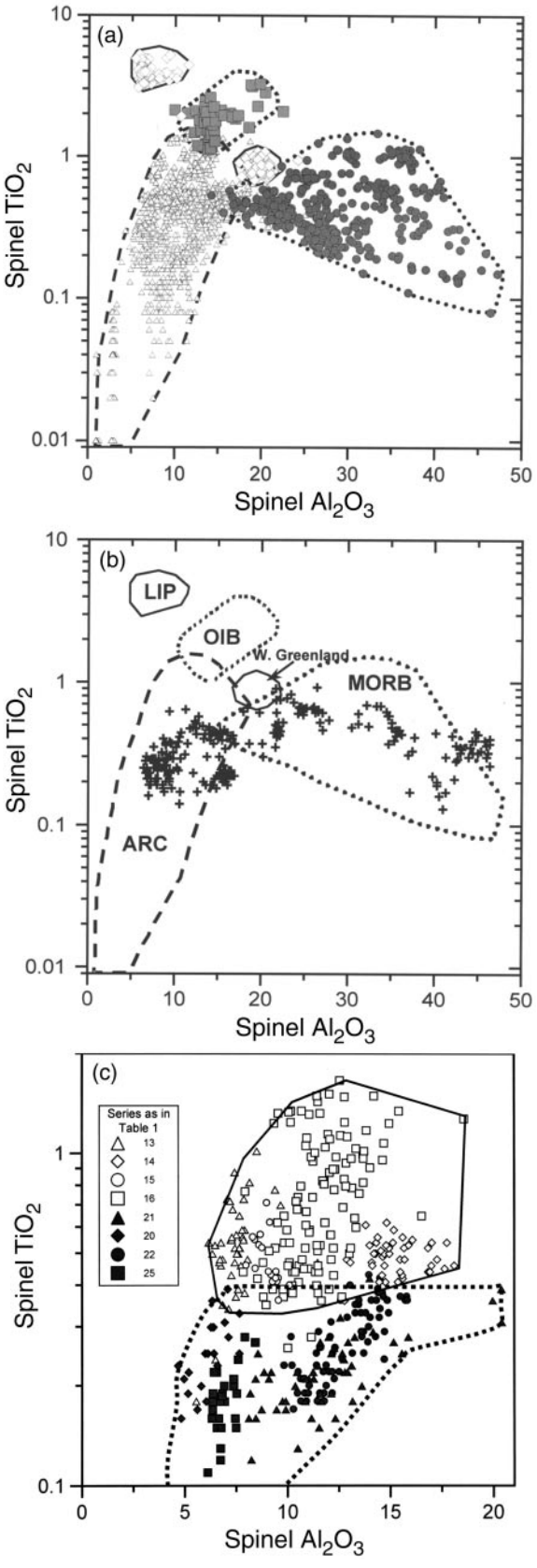

Fig. 5. Al_2O_3 vs TiO_2 compositional relationships in spinel inclusions trapped in primitive olivine Fo >84: (a) discrimination between mid-ocean ridge basalt (MORB, grey circles), ocean-island basalt (OIB, grey squares), large igneous province (LIP, ◇) and island-arc magmas (ARC, △); (b) spinels from modern back-arc settings show both island-arc and MORB affinities; (c) discrimination between lower-Ti (boninites and tholeiites) and higher-Ti (calc-alkaline and high-K) island-arc series.

petrological and geochemical data, including TiO_2 abundances in spinel. Spinel Al_2O_3 abundances depend on the melt composition (Fig. 4), which is a function of pressure, temperature, and degree of partial melting, as well as source chemical and phase compositions. We emphasize here that the compositions of spinel from LIP, OIB and MORB form a continuum on Al_2O_3 vs TiO_2 diagram (Fig. 5a), which extends from the high-Ti, low-Al corner (LIP) to the low-Ti, high-Al end (MORB). This trend is coincident with pronounced changes in the mantle petrological–geochemical characteristics (fertile–enriched to refractory–depleted) and conditions (pressure and temperature) of mantle melting. Pressure and temperature vary from high [e.g. >60 kbar and >1800°C for Siberian meimechites (Sobolev *et al.*, 1992)] through moderate [e.g. 20–40 kar and 1450–1600°C for Hawaiian and West Greenland magmas (Eggins, 1992; Sobolev & Nikogosian, 1994; Gill *et al.*, 1995)] to low values [e.g. 2–22 kbar and 1200–1450°C for mid-ocean ridge primary melts (Danyushevsky *et al.*, 1987; Falloon & Green, 1988; Kinzler & Grove, 1992; Sobolev & Shimizu, 1993)]. As expected, these variations in conditions of melting coincide with changes in magma chemistry, with abundances of Mg, Fe and Ti decreasing, and Si and Al increasing along the trend.

Using the analogy with LIP and OIB spinel, low Al_2O_3 abundance in island-arc spinels may suggest that their parental magmas were also high-Mg high-temperature liquids formed at elevated pressures. This is in agreement with estimates of pressure and temperature of the mantle source for a number of island-arc magmas: for example, East Kamchatka [30–50 kbar, 1500–1700°C (Kamenetsky *et al.*, 1995*b*)], Tonga [20–25 kbar, 1450–1550°C (Sobolev & Danyushevsky, 1994)], Troodos Upper Pillow Lavas [20–30 kbar, 1380–1550°C (Sobolev *et al.*, 1993)], and Vanuatu [30 kbar, 1300°C (Eggins, 1993)].

The use of spinel chemistry: examples from volcanisedimentary and ancient rocks

Volcaniclastic rocks may have multiple and variable sources. In these rocks detrital spinel may be the only primary igneous mineral not affected by alteration and, therefore, it can provide valuable petrological information. Compositions of detrital spinel may help to recognize and identify the chemical affinity and tectonic provenance of the source rocks.

The discrimination between 'mantle' and volcanic spinel is the first step in constraining the spinel compositional populations. We have shown above that spinels from mantle peridotites tend to have statistically lower *mg*-number than spinel coexisting with primitive olivine (Fo >88) from volcanic rocks (Fig. 3c). However, this criterion is effectively irrelevant for sediments, as olivine is rarely preserved. The more useful variables are TiO_2 and Fe^{2+}/Fe^{3+} in spinel. 'Mantle' spinels have statistically lower TiO_2 (<0·2 wt %) and higher Fe^{2+}/Fe^{3+} (>2) over the whole interval in Al_2O_3 (6–56 wt %) than volcanic spinels, though low-Ti compositions (TiO_2 <0·2 wt %) high Fe^{2+}/Fe^{3+} (up to four) compositions also exist among volcanic boninitic and arc tholeiitic spinels (Fig. 6). Compositions of 'mantle' spinels can be subdivided into two broadly overlapping fields (Fig. 6) represented by spinel from suprasubduction zone peridotites (lower Al_2O_3) and spinel from MORB-type peridotites (higher Al_2O_3). The compositional affinities of volcanic spinel can be evaluated using the data from Figs 4 and 5.

To demonstrate how spinel composition can be used to unravel the tectonic evolution and petrogenesis of altered volcanic and sedimentary rocks in ancient fold belts we present a summary of a study where spinel chemistry has provided valuable information. The Lachlan Fold Belt (LFB) in southeastern Australia contains Cambrian to Devonian volcanic and sedimentary rocks intruded by Silurian and Devonian granitoids (Coney, 1992). The Ordovician rocks of the LFB consist of two contrasting assemblages, quartz-rich continental-derived turbidites, and medium- to high-K volcanics and volcaniclastics. The genetic relationship between these two sequences has long been a problem as the majority of their contacts are fault bounded. The Snowy Mountains terrain is located in the central LFB. It contains a thin block of Ordovician volcaniclastic rocks interbedded with minor volcanics in faulted contact with Ordovician quartz-rich sandstones. The faults on either side of the volcaniclastic rocks contain ophiolitic fragments. The fault to the east contains altered pillow basalts, cherts, meta-dolerite and hyaloclastites. The fault to the west contains serpentinite, meta-dolerite and altered basalts.

The chemistry of spinels from the ophiolitic fragments and volcaniclastic rocks provides important constraints on the relationship between the Ordovician quartz-rich and volcaniclastics sequences. Spinels from a hyaloclastite from the eastern fault have high Al_2O_3 similar to those from MORB or MORB-type back-arc rocks, indicating that they crystallized from a melt containing between 14 and 16 wt % Al_2O_3 (Fig. 7). In contrast, spinels from serpentinites in the western fault zone are low in both TiO_2 and Al_2O_3, indicating that these rocks are fragments of suprasubduction zone mantle peridotites. It is therefore unlikely that the rocks in both fault zones could be derived from a single ophiolite. Spinels from the volcaniclastic sequence have low Al_2O_3 and moderate TiO_2 (Fig. 7), indicating that they crystallized from a melt containing between 10 and 11 wt % Al_2O_3. This melt composition is similar to that of the most primitive shoshonitic basalts, which are interbedded with the volcaniclastic rocks. The spinels were therefore derived locally from the erosion

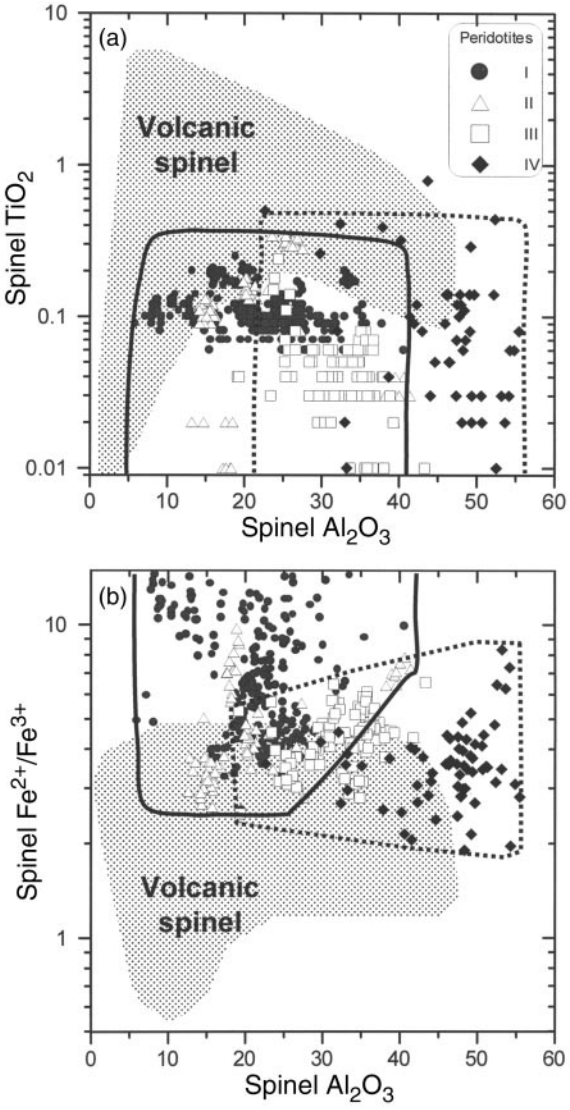

Fig. 6. Discrimination between volcanic and 'mantle' spinel using TiO_2 (a) and Fe^{2+}/Fe^{3+} (b). Symbols as in Fig. 3c. Continuous and dashed lines enclose compositions from suprasubduction zone and MORB-type peridotites, respectively.

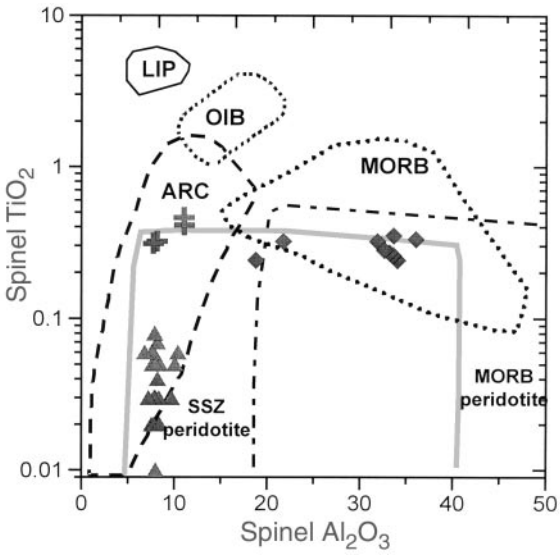

Fig. 7. Al_2O_3 vs TiO_2 compositional relationships in spinel from the Snowy Mountains rocks (Ordovician Lachlan Fold Belt, SE Australia). Spinels are from volcaniclastic sandstone (grey crosses), hyaloclastite (grey diamonds) and serpentinites (grey triangles) are compared with compositional fields of spinel from volcanic rocks and mantle peridotites (see Figs 5 and 6a).

of the basalts and not from erosion of the ophiolitic rocks within the fault zones on either side.

The chemistry of the spinels from the Snowy Mountains shows that the Late Ordovician volcaniclastics are separated from the Early Ordovician quartz-rich turbidites by both MORB-type and SSZ-type ophiolites. This suggests that the sedimentary rocks originated from shoshonitic volcanics in a separate tectonic environment to the continental turbidites and were juxtaposed during either strike-slip tectonics and/or the closure of major oceanic basins.

CONCLUSIONS

At magmatic conditions, spinel *mg*-number is a function of melt *mg*-number and Al_2O_3, whereas at near- and post-magmatic conditions it is controlled by the rate of cooling and re-equilibration with the silicates. Within a given volcanic suite, spinel *mg*-number can be used as a measure of the extent of crystal fractionation. The *mg*-number–*cr*-number relationships in spinel from altered volcanic rocks or sediments can help to approximate compositions of olivine, which once coexisted with spinel.

Abundances of Al_2O_3 and TiO_2 in magmatic spinel are mainly controlled by contents of these oxides in the parental melts, and thus can be used to discriminate between different magma types, their tectonic affinities and mantle sources. The application of spinel Al_2O_3 (*cr*-number) alone to directly constrain the mantle source composition is not confirmed in this study.

The compositional features of spinel and the differences in TiO_2 and Fe^{2+}/Fe^{3+} between magmatic and mantle spinel can be used in characterizing altered magmatic rocks, and the sources of detrital spinels in clastic sedimentary rocks, thus contributing to the understanding of the tectonic development of source geological terrains.

ACKNOWLEDGEMENTS

The authors are indebted to Maya Kamenetsky, who made this study possible by patiently separating, mounting and polishing a myriad of olivine and spinel grains.

Microprobe work was assisted by I. Sigurdsson, N. Kononkova, W. Jablonski, and D. Steele. We would like to thank H. Bougault, J. W. Bristow, W. E. Cameron, S.-L. Chung, R. Clocchiatti, D. H. Green, B. J. Griffin, S. Eggins, R. Hekinian, N. Métrich, R. Mühe, A. K. Pedersen, A. P. le Roex, R. Shinjo, A. Sobolev, S. Zlobin, and many others for providing samples of spinel-bearing rocks. Special thanks go to K. Stait for keeping the rockstore of the University of Tasmania in perfect order. Hugh O'Neill and Greg Yaxley helped with some heating experiments. We appreciate numerous discussions with M. Portnyagin, L. Danyushevsky, A. Sobolev, F. Della-Pasqua, A. Gurenko, G. Yaxley and M. Gasparon. Steve Eggins and Leonid Danyushevsky refined our understanding of spinel–olivine re-equilibration. We thank Leonid Danyushevsky for comments on an earlier version of this paper, and Steve Barnes and Brent McInnes for formal reviews. This work was funded by ARC Large Grants to A.J.C., an ARC Research Fellowship Grant to V.S.K. and funding from the Australian Research Council's Research Centres Program.

REFERENCES

Allan, J. F. (1992). Cr-spinel as a petrogenetic indicator: deducing magma composition from spinels in highly altered basalts from the Japan Sea, Sites 794 and 797. In: Tamaki, K., Suyehiro, K., Allan, J., McWilliams, M., *et al.* (eds) *Proceedings of the Ocean Drilling Program, Scientific Results, 127/128 (Part 2)*. College Station, TX: Ocean Drilling Program, pp. 837–847.

Allan, J. F. (1994). Cr-spinel in depleted basalts from the Lau Basin backarc, ODP Leg 135; petrogenetic history from Mg–Fe crystal–liquid exchange. In: Hawkins, J. W., Parson, L. M., Allan, J. F., *et al.* (eds) *Proceedings of the Ocean Drilling Program, Scientific Results, 135*. College Station, TX: Ocean Drilling Program, pp. 565–584.

Allan, J. F., Sack, R. O. & Batiza, R. (1988). Cr-rich spinels as petrogenetic indicators: MORB-type lavas from the Lamont seamount chain, eastern Pacific. *American Mineralogist* **73**, 741–753.

Arai, S. (1987). An estimation of the least depleted spinel peridotite on the basis of olivine–spinel mantle array. *Neues Jahrbuch für Mineralogie, Monatshefte* **8**, 347–354.

Arai, S. (1992). Chemistry of chromian spinel in volcanic rocks as a potential guide to magma chemistry. *Mineralogical Magazine* **56**, 173–184.

Arai, S. (1994*a*). Characterization of spinel peridotites by olivine–spinel compositional relationships: review and interpretation. *Chemical Geology* **113**, 191–204.

Arai, S. (1994*b*). Compositional variation of olivine–chromian spinel in Mg-rich magmas as a guide to their residual spinel peridotites. *Journal of Volcanology and Geothermal Research* **59**, 279–293.

Ballhaus, C., Berry, R. F. & Green, D. H. (1991). High pressure experimental calibration of the olivine–orthopyroxene–spinel oxygen geobarometer: implications for the oxidation state of the upper mantle. *Contributions to Mineralogy and Petrology* **107**, 27–40.

Barnes, S. J. (1998). Chromite in komatiites, 1. Magmatic controls on crystallization and composition. *Journal of Petrology* **39**, 1689–1720.

Barsdell, M. (1988). Petrology and petrogenesis of clinopyroxene-rich tholeiitic lavas, Merelava volcano, Vanuatu. *Journal of Petrology* **29**, 927–964.

Basylev, B. A. & Kamenetsky, V. S. (1998). Genesis of peridotites from the ophiolite complex of Macquarie Island, southwestern Pacific Ocean. *Petrology* **6**, 335–350.

Bonatti, E. & Michael, P. J. (1989). Mantle peridotites from continental rifts to ocean basins to subduction zones. *Earth and Planetary Science Letters* **91**, 297–311.

Bristow, J. W. (1984). Picritic rocks of the north Lebombo and south-east Zimbabwe. In: Erlank, A. J. (ed.) *Petrogenesis of the Volcanic Rocks of the Karoo Province. South Africa Geological Society, Special Publication* **13**, 105–123.

Cameron, W. E. (1989). Contrasting boninite–tholeiite associations from New Caledonia. In: Crawford, A. J. (ed.) *Boninites*. London: Unwin Hyman, pp. 314–338.

Chung, S.-L. & Jahn, B.-m. (1995). Plume–lithosphere interaction in generation of the Emeishan flood basalts at the Permian–Triassic boundary. *Geology* **23**, 889–892.

Clynne, M. A. & Borg, L. E. (1997). Olivine and chromian spinel in primitive calc-alkaline and tholeiitic lavas from the southernmost Cascade Range, California: a reflection of relative fertility of the source. *Canadian Mineralogist* **35**, 453–472.

Coney, P. J. (1992). The Lachlan belt of eastern Australia and Circum-Pacific tectonic evolution. *Tectonophysics* **214**, 1–25.

Crawford, A. J. (1980). A clinoenstatite-bearing cumulate olivine pyroxenite from Howqua, Victoria. *Contributions to Mineralogy and Petrology* **75**, 353–367.

Danyushevsky, L. V. (1995). Spinels as geochemical and petrological indicators of arc magma genesis. In: Barnes, H. L. (ed.) *V. M. Goldschmidt Conference Abstracts*, Geochemical Society, 40.

Danyushevsky, L. V., Sobolev, A. V. & Dmitriev, L. V. (1987). Low-titanium orthopyroxene-bearing tholeiite, a new type of ocean-rift tholeiite. *Transactions (Doklady) of the USSR Academy of Sciences* **292**, 102–105.

Danyushevsky, L. V., Sobolev, A. V. & Falloon, T. J. (1995). North Tongan high-Ca boninite petrogenesis: the role of Samoan plume and subduction zone–transform fault transition. *Journal of Geodynamics* **20**, 219–241.

Della-Pasqua, F. N. & Varne, R. (1997). Primitive ankaramitic magmas in volcanic arcs: a melt-inclusion approach. *Canadian Mineralogist* **35**, 291–312.

Della-Pasqua, F. N., Kamenetsky, V. S., Gasparon, M., Crawford, A. J. & Varne, R. (1995). Al-rich spinel in primitive arc volcanics. *Mineralogy and Petrology* **53**, 1–26.

Dick, H. J. B. (1989). Abyssal peridotites, very slow spreading ridges and ocean ridge magmatism. In: Saunders, A. D. & Norry, M. J. (eds) *Magmatism in the Ocean Basins. Geological Society, London, Special Publication* **42**, 71–105.

Dick, H. J. B. & Bullen, T. (1984). Chromian spinel as a petrogenetic indicator in abyssal and alpine-type peridotites and spatially associated lavas. *Contributions to Mineralogy and Petrology* **86**, 54–76.

Dmitriev, L. V., Magakyan, R., Danyushevsky, L. V., Kamenetsky, V. S. & Kononkova, N. N. (1991). New data on primitive tholeiites from oceanic crust of the Atlantic (from materials of 12 cruise of R/V *Academician B. Petrov*). *Vulkanologiya i Seismologiya* 78–94.

Dril, S. I., Kuzmin, M. I., Tsipukova, S. S. & Zonenshain, L. P. (1997). Geochemistry of basalts from the western Woodlark, Lau and Manus basins: implications for their petrogenesis and source rock compositions. *Marine Geology* **142**, 57–83.

Duncan, R. A. & Green, D. H. (1987). The genesis of refractory melts in the formation of oceanic crust. *Contributions to Mineralogy and Petrology* **96**, 326–342.

Eggins, S. M. (1992). Petrogenesis of Hawaiian tholeiites: 1, phase equilibria constraints. *Contributions to Mineralogy and Petrology* **110**, 387–397.

Eggins, S. M. (1993). Origin and differentiation of picritic arc magmas, Ambae (Aoba), Vanuatu. *Contributions to Mineralogy and Petrology* **114**, 79–100.

Evans, B. W. & Frost, B. R. (1975). Chrome spinel in progressive metamorphism—a preliminary analysis. *Geochimica et Cosmochimica Acta* **39**, 959–972.

Falloon, T. J. & Green, D. H. (1988). Anhydrous partial melting of peridotite from 8 to 35 kb and the petrogenesis of MORB. *Journal of Petrology* **29**, 379–414.

Fisk, M. R. & Bence, A. E. (1980). Experimental crystallization of chrome spinel in FAMOUS basalt 527-1-1. *Earth and Planetary Science Letters* **48**, 111–123.

Gill, R. C. O., Holm, P. M. & Nielsen, T. F. D. (1995). Was a short-lived Baffin Bay plume active prior to initiation of the present Icelandic plume? Clues from the high-Mg picrites of West Greenland. *Lithos* **34**, 27–39.

Gioncada, A., Clocchiatti, R., Sbrana, A., Bottazzi, P., Massare, D. & Ottolini, L. (1998). A study of melt inclusions at Vulcano (Aeolian Islands, Italy): insights on the primitive magmas and on the volcanic feeding system. *Bulletin of Volcanology* **60**, 286–306.

Gurenko, A. A., Sobolev, A. V. & Kononkova, N. N. (1992). New petrological data on Icelandic rift alkali basalts. *Geochemistry International* **29**, 41–53.

Hill, R. & Roeder, P. (1974). The crystallization of spinel from basaltic liquid as a function of oxygen fugacity. *Journal of Geology* **82**, 709–729.

Holm, P. M., Gill, R. C. O., Pedersen, A. K., Larsen, J. G., Hald, N., Nielsen, T. F. D. & Thirlwall, M. F. (1993). The Tertiary picrites of West Greenland: contributions from 'Icelandic' and other sources. *Earth and Planetary Science Letters* **115**, 227–244.

Irvine, T. N. (1965). Chromian spinel as a petrogenetic indicator. Part I. Theory. *Canadian Journal of Earth Sciences* **2**, 648–671.

Irvine, T. N. (1967). Chromian spinel as a petrogenetic indicator. Part 2. Petrologic applications. *Canadian Journal of Earth Sciences* **4**, 71–103.

Ishii, T., Robinson, P. T., Maekawa, H. & Fiske, R. (1992). Petrological studies of peridotites from diapiric serpentinite seamounts in the Isu–Ogasawara–Mariana forearc, Leg 125. In: Fryer, P., Pearce, J. A., Stokking, L. B., *et al.* (eds) *Proceedings of the Ocean Drilling Program, Scientific Results, 125*. College Station, TX: Ocean Drilling Program, pp. 445–485.

Jaques, A. L. & Green, D. H. (1980). Anhydrous melting of peridotite at 0–15 kb pressure and the genesis of tholeiitic basalts. *Contributions to Mineralogy and Petrology* **73**, 287–310.

Kamenetsky, V. (1996). Methodology for the study of melt inclusions in Cr-spinel, and implications for parental melts of MORB from FAMOUS area. *Earth and Planetary Science Letters* **142**, 479–486.

Kamenetsky, V. & Clocchiatti, R. (1996). Primitive magmatism of Mt Etna: insights from mineralogy and melt inclusions. *Earth and Planetary Science Letters* **142**, 553–572.

Kamenetsky, V. & Crawford, A. J. (1998). Melt–peridotite reaction recorded in the chemistry of spinel and melt inclusions in basalt from 43°N, Mid-Atlantic Ridge. *Earth and Planetary Science Letters* **164**, 345–352.

Kamenetsky, V. S., Portnyagin, M. V., Sobolev, A. V. & Danyushevsky, L. V. (1993). Magma composition and crystallization conditions of the picrite–basalt suite in the Tumrok Range, East Kamchatka. *Geochemistry International* **30**, 58–73.

Kamenetsky, V., Métrich, N. & Cioni, R. (1995*a*). Potassic primary melts of Vulsini (Roman Province): evidence from mineralogy and melt inclusions. *Contributions to Mineralogy and Petrology* **120**, 186–196.

Kamenetsky, V. S., Sobolev, A. V., Joron, J.-L. & Semet, M. P. (1995*b*). Petrology and geochemistry of Cretaceous ultramafic volcanics from East Kamchatka. *Journal of Petrology* **36**, 637–662.

Kamenetsky, V. S., Crawford, A. J., Eggins, S. M. & Mühe, R. (1997). Phenocrysts and melt inclusion chemistry of near-axis seamounts, Valu Fa Ridge, Lau Basin: insight into mantle wedge melting and the addition of subduction components. *Earth and Planetary Science Letters* **151**, 205–223.

Kamenetsky, V. S., Eggins, S. M., Crawford, A. J., Green, D. H., Gasparon, M. & Falloon, T. J. (1998). Calcic melt inclusions in primitive olivine at 43°N MAR: evidence for melt–rock reaction/melting involving clinopyroxene-rich lithologies during MORB generation. *Earth and Planetary Science Letters* **160**, 115–132.

Kamenetsky, V. S., Everard, J. L., Crawford, A. J., Varne, R., Eggins, S. M. & Lanyon, R. (2000). Enriched end-member of primitive MORB melts: petrology and geochemistry of glasses from Macquarie Island (SW Pacific). *Journal of Petrology* **41**, 411–430.

Kinzler, R. J. & Grove, T. L. (1992). Primary magmas of mid-ocean ridge basalts 2. Applications. *Journal of Geophysical Research* **97**, 6907–6926.

Langmuir, C. H., Bender, J. F., Bence, A. E., Hanson, G. N. & Taylor, S. R. (1977). Petrogenesis of basalts from the FAMOUS area: Mid-Atlantic Ridge. *Earth and Planetary Science Letters* **36**, 133–156.

Leblanc, M. (1995). Chromitite and ultramafic rock compositional zoning through a paleotransform fault, Poum, New Caledonia. *Economic Geology* **90**, 2028–2039.

le Roex, A. P., Dick, H. J. B., Gulen, L., Reid, A. M. & Erlank, A. J. (1987). Local and regional heterogeneity in MORB from the Mid-Atlantic Ridge between 54·5°S and 51°S: evidence for geochemical enrichment. *Geochimica et Cosmochimica Acta* **51**, 541–555.

Lightfoot, P. C., Hawkesworth, C. J., Olshefsky, K., Green, T., Doherty, W. & Keays, R. R. (1997). Geochemistry of Tertiary tholeiites and picrites from Qeqertarssuaq (Disko Island) and Nuussuaq, West Greenland with implications for the mineral potential of comagmatic intrusions. *Contributions to Mineralogy and Petrology* **128**, 139–163.

Maillet, P., Ruellan, E., Gerard, M., Person, A., Bellon, H., Cotten, J., Joron, J.-L., Nakada, S. & Price, R. C. (1995). Tectonics, magmatism, and evolution of the New Hebrides backarc troughs (southwest Pacific). In: Taylor, B. (ed.) *Backarc Basins: Tectonics and Magmatism*. New York: Plenum, pp. 177–235.

Maurel, C. & Maurel, P. (1982*a*). Étude expérimentale de la distribution de l'aluminium entre bain silicate basique et spinelle chromifère. Implications pétrogenetiques: teneur en chrome des spinelles. *Bulletin de Minéralogie* **105**, 197–202.

Maurel, C. & Maurel, P. (1982*b*). Étude expérimentale de l'équilibre Fe^{2+}–Fe^{3+} dans les spinelles chromifères et les liquides silicates basiques coexistants, à 1 atm. *Comptes Rendus de l'Académie des Sciences* **295**, 209–212.

Maury, R. C., Elazzouzi, M., Bellon, H., Liotard, J. M., Guille, G., Barsczus, H. G., Chauvel, C., Diraison, C., Dupuy, C., Vidal, P. & Brousse, R. (1994). Geology and petrology of Tubuai (Austral Islands, French Polynesia.) *Comptes Rendus de l'Académie des Sciences* **318**, 1341–1347.

McNeill, A. W. (1997). The crystallisation history of normal mid-ocean ridge basalts from the eastern Pacific Ocean and implications for the composition of primary mid-ocean ridge magmas: evidence from mineralogy, pillow-rim glasses and melt inclusion studies. Ph.D. thesis, University of Tasmania.

Monzier, M., Danyushevsky, L. V., Crawford, A. J., Bellon, H. & Cotten, J. (1993). High-Mg andesites from the southern termination of the New Hebrides island arc (SW Pacific). *Journal of Volcanology and Geothermal Research* **57**, 193–217.

Monzier, M., Robin, C., Eissen, J. P. & Cotten, J. (1997). Geochemistry vs. seismo-tectonics along the volcanic New Hebrides Central Chain (Southwest Pacific). *Journal of Volcanology and Geothermal Research* **78**, 1–29.

Murck, B. W. & Campbell, I. H. (1986). The effects of temperature, oxygen fugacity and melt composition on the behavior of chromium in basic and ultrabasic melts. *Geochimica et Cosmochimica Acta* **50**, 1871–1887.

Natland, J. H., Adamson, A. C., Laverne, C., Melson, W. G. & O'Hearn, T. (1983). A compositionally nearly steady-state magma chamber at the Costa Rica Rift: evidence from basalt glass and mineral data, Deep Sea Drilling Project Sites 501, 504 and 505. In: Cann, J. R., Langseth, M., Honnorez, J., Von Herzen, R. P., White, S. M., *et al.* (eds) *Initial Reports of the Deep Sea Drilling Project, 69*. Washington, DC: US Government Printing Office, pp. 811–859.

Ozawa, K. (1984). Olivine–spinel geospeedometry: analysis of diffusion-controlled Mg–Fe^{2+} exchange. *Geochimica et Cosmochimica Acta* **48**, 2597–2611.

Picard, C., Monzier, M., Eissen, J.-P. & Robin, C. (1995). Concomitant evolution of tectonic environment and magma geochemistry, Ambrym volcano (Vanuatu, New Hebrides arc). In: Smellie, J. L. (ed.) *Volcanism Associated with Extension at Consumed Plate Margins. Geological Society, London, Special Publication* **81**, 135–154.

Roeder, P. L. (1994). Chromite: from the fiery rain of chondrules to the Kilauea Iki lava lake. *Canadian Mineralogist* **32**, 729–746.

Roeder, P. L. & Campbell, I. H. (1985). The effect of postcumulus reactions on compositions of chrome-spinels from the Jimberlana Intrusion. *Journal of Petrology* **26**, 763–786.

Roeder, P. L. & Reynolds, I. (1991). Crystallisation of chromite and chromium solubility in basaltic melts. *Journal of Petrology* **32**, 909–934.

Sack, R. O. (1982). Spinels as petrogenetic indicators: activity–composition relations at low pressures. *Contributions to Mineralogy and Petrology* **79**, 169–186.

Sack, R. O. & Ghiorso, M. S. (1991). Chromian spinels as petrogenetic indicators: thermodynamics and petrological applications. *American Mineralogist* **76**, 827–847.

Scowen, P. A. H., Roeder, P. L. & Helz, R. T. (1991). Reequilibration of chromite within Kilauea Iki lava lake, Hawaii. *Contributions to Mineralogy and Petrology* **107**, 8–20.

Shibata, T., Thompson, G. & Frey, F. A. (1979). Tholeiitic and alkali basalts from the Mid-Atlantic Ridge at 43°N. *Contributions to Mineralogy and Petrology* **70**, 127–141.

Shinjo, R., Chung, S. L., Kato, Y. & Kimura, M. (1999). Geochemical and Sr–Nd isotopic characteristics of volcanic rocks from the Okinawa Trough and Ryukyu Arc: implications for the evolution of a young, intracontinental back arc basin. *Journal of Geophysical Research* **104**, 10591–10608.

Sigurdsson, H. (1977). Spinels in leg 37 basalts and peridotites: phase chemistry and zoning. In: Aumento, F., Melson, W. G., Hall, J. M., *et al.* (eds) *Initial Reports of the Deep Sea Drilling Project, 37*. College Station, TX: Ocean Drilling Program, pp. 883–891.

Sigurdsson, H. & Schilling, J.-G. (1976). Spinels in Mid-Atlantic Ridge basalts: chemistry and occurrence. *Earth and Planetary Science Letters* **29**, 7–20.

Sigurdsson, I. A., Kamenetsky, V. S., Crawford, A. J., Eggins, S. M. & Zlobin, S. K. (1993). Primitive island arc and oceanic lavas from the Hunter ridge–Hunter fracture zone. Evidence from glass, olivine and spinel compositions. *Mineralogy and Petrology* **47**, 149–169.

Sobolev, A. V. & Danyushevsky, L. V. (1994). Petrology and geochemistry of boninites from the north termination of the Tonga Trench: constraints on the generation conditions of primary high-Ca boninite magmas. *Journal of Petrology* **35**, 1183–1213.

Sobolev, A. V. & Nikogosian, I. K. (1994). Petrology of long-lived mantle plume magmatism: Hawaii, Pacific and Reunion Island, Indian Ocean. *Petrology* **2**, 111–144.

Sobolev, A. V. & Shimizu, N. (1993). Ultra-depleted primary melt included in an olivine from the Mid-Atlantic Ridge. *Nature* **363**, 151–154.

Sobolev, A. V., Dmitriev, L. V., Barsukov, V. L., Nevsorov, V. N. & Slutsky, A. B. (1980). The formation conditions of high magnesium olivines from the monomineral fraction of Luna-24 regolith. In: Criswell, P. R. & Merrill, R. B. (eds) *Igneous Processes and Remote Sensing*. New York: Pergamon. *Proceedings of the 11th Lunar and Planetary Science Conference. Geochimica et Cosmochimica Acta Supplement* 105–116.

Sobolev, A. V., Kamenetsky, V. S. & Kononkova, N. N. (1992). New data on Siberian meymechite petrology. *Geochemistry International* **29**, 10–20.

Sobolev, A. V., Portnyagin, M. V., Dmitriev, L. V., Tsameryan, O. P., Danyushevsky, L. V., Kononkova, N. N., Shimizu, N. & Robinson, P. T. (1993). Petrology of ultramafic lavas and associated rocks of the Troodos massif, Cyprus. *Petrology* **1**, 331–361.

Sobolev, A. V., Kamenetsky, V. S. & Crawford, A. J. (1995). Very hot H_2O-bearing Phanerozoic mantle: evidence from ultramafic melt inclusions in phenocrysts from Papua-New Guinea. *EOS Transactions, American Geophysical Union* **76**, S270.

Thy, P. (1983). Spinel minerals in transitional and alkali basaltic glasses from Iceland. *Contributions to Mineralogy and Petrology* **83**, 141–149.

Walker, D. A. & Cameron, W. E. (1983). Boninite primary magmas: evidence from Cape Vogel Peninsula, PNG. *Contributions to Mineralogy and Petrology* **83**, 150–158.

Woodhead, J. D. (1996). Extreme HIMU in oceanic setting: the geochemistry of Mangaia Island (Polynesia), and temporal evolution of the Cook–Austral hotspot. *Journal of Volcanology and Geothermal Research* **72**, 1–19.

Zlobin, S. K., Kamenetsky, V. S., Sobolev, A. V. & Kononkova, N. N. (1991). Chrome spinel inclusion data on the parent melt for the parallel-dike complex in the Mainits-zone ophiolites in the Koryak uplands. *Geochemistry International* **28**, 68–77.